ELSEVIER

Journal of Structural Geology 27 (2005) 2099–2112

JOURNAL OF STRUCTURAL GEOLOGY

www.elsevier.com/locate/jsg

Comparison of structural features of the fault zone developed at different protoliths: crystalline rocks and mudrocks

Hee-Kwon Lee*, Hyeong Soo Kim[1]

Department of Geology, Kangwon National University, Chunchon, Kangwon-Do 200-701, Republic of Korea

Received 25 August 2003; received in revised form 6 May 2005; accepted 13 June 2005
Available online 15 August 2005

Abstract

We investigated the mesoscopic and microscopic structural features of the Keumwang fault zone, Korea, to determine the effect of different protoliths (crystalline granitic gneiss and mudrock) on fault zone structure including discrete shear surfaces, shear bands, foliation, porphyroclasts and calcite veins. Overall, in crystalline rock, the shear deformation tends to be localized to a fault core or several fault gouge-dominated layers within the fault zone. The cataclastic flow appears to become stronger toward the fault core. Most of the shear deformation appears to be partitioned between slip on discrete shear surfaces and shear bands, and cataclastic flow, including syntectonic alteration in the fine-grained matrix of fault rocks. In contrast, within mudrocks, shear deformation tends to be relatively uniformly distributed within the entire fault zone. Shearing generates continuous *S*-foliations throughout the whole fault zone. Most of the shearing is accommodated by slip along these foliations and on discrete shear surfaces distributed within the entire fault zone.

Keywords: Faults; Gouge; Cataclasite; Brittle fault zone; Shear surface; Foliation

1. Introduction

The deformation of rocks in the crust is very inhomogeneous, being either distributed or concentrated in the ductile shear zones or brittle fault zones (Mitra, 1992). Brittle fault zones are often characterized by a fault core of highly crushed rock bounded by damaged host-rocks containing fault breccia, fractures, subsidiary faults and veins (Flinn, 1977; House and Gray, 1982; Wojtal and Mitra, 1986; Chester and Logan, 1987; Lee and Schwarcz, 1996; Schulz and Evans, 2000). Structural features developed in brittle fault zones are controlled by various factors including lithology, fault scale, tectonic setting, deformation history and fluid chemistry (Goddard and Evans, 1995; Caine et al., 1996; Wibberley, 1999; Schulz and Evans, 2000). Studies of fault rocks formed at shallow crustal levels show that feldspar grains are weaker than quartz grains and chemical reactions between feldspars and fluid result in strain softening (Evans, 1988; Chester et al., 1993; Evans and Chester, 1995; Wibberley, 1999).

Several researchers have investigated characteristic structural features and evolution of fault zones developed in crystalline rocks (Chester and Logan, 1987; Chester et al., 1993; Evans and Chester, 1995) and porous sandstones (Aydin and Johnson, 1983; Shipton and Cowie, 2001). However, studies of the characteristic structural features of a brittle fault zone developed in mudrocks are lacking. The goal of this study is to characterize the effect of protolith type on the structure of brittle fault zones. In particular, we investigate the structure of a single fault that juxtaposes crystalline rock and mudrock, to understand the effect of the protolith.

We first undertook a qualitative description of fault-related structures to characterize the deformation of the brittle fault zone. We then quantified the observations in order to understand the spatial variations of structural features within the fault zone. About 4–10 measurements of planar structures such as shear surfaces, shear bands and foliation were made at every 50 cm along the scan line

* Corresponding author. Tel.: +82 33 250 8558; fax: +82 33 242 8550.
E-mail addresses: heekwon@kangwon.ac.kr (H.-K. Lee), hskim@knu.ac.kr (H.S. Kim).
[1] Present address: Department of Earth Science Education, Kyungpook National University, Daeku, Kyungsangbuk-Do 702-701, Republic of Korea.

0191-8141/$ - see front matter © 2005 Elsevier Ltd. All rights reserved.
doi:10.1016/j.jsg.2005.06.012

perpendicular to the planar structures in the exposures. We used the directional nomenclature of structural features following the terminology of Rutter et al. (1986) and Passchier and Trouw (1996). At one location, grain size was determined by optically measuring the long dimension of grains under the cross-hairs for 300 grains in each thin section. Modal analysis was conducted under the petrographic microscope to determine the change of mineral composition from protolith to fault core. XRD and XRF analyses were used to characterize the geochemistry of the fault zone. X-ray diffractometer (XRD) analyses were conducted to compare mineral composition of clay-bearing fault gouge to that of fine-grained matrix of cataclasite. Major element analysis for fault rocks derived from the granitic gneiss was also performed using a Philips PW 2400 X-ray fluorescence spectrometer. We observed microstructures in the fine-grained matrix of cataclasite using a JEOL JSM-5410 scanning electron microprobe (SEM).

We have examined the variations of mesoscopic and microscopic structural features along four traverses across

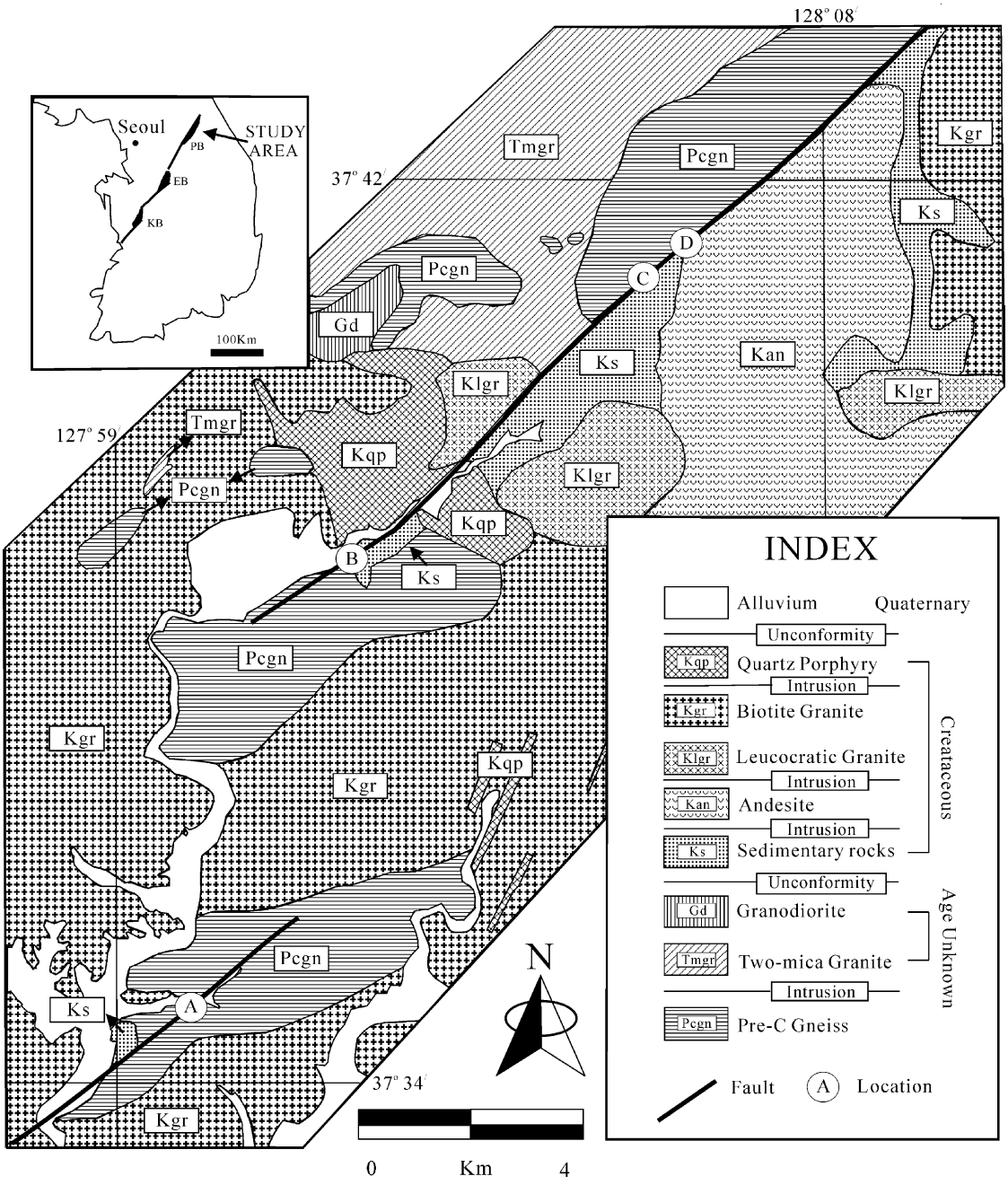

Fig. 1. Geologic map of the study area showing the locations of localities A, B, C and D along the Keumwang fault zone. Inset map shows the study area and the Cretaceous sedimentary basins developed along the Kongju fault system. Cretaceous Basins: KB, Kongju Basin; EB, Eumseong Basin; PB, Pungam Basin.

the Keumwang fault zone, Korea, to investigate the effect of different protoliths (mudrock and crystalline granitic gneiss) on structural features associated with strike-slip fault movements. We also characterized the variations of grain size, mineralogy and geochemistry along one traverse across the Keumwang fault zone in the Precambrian granitic gneiss to determine the deformation mechanisms operative in the fault zone.

2. Geological setting

The Keumwang fault zone is a segment of the Kongju fault system, which cuts the Korean peninsula with NE–SW strike (Fig. 1). The Kongju fault system was activated by left-lateral movements in the Late Jurassic to the Cretaceous, forming small-scale basins along the fault system. These basins were filled with a thick sequence of sediments during the Early to Late Cretaceous. During and after deposition, the Kongju fault system was sporadically active along the northwestern margin of the basins (Chough et al., 2000). Geological structures in the basins are characterized by en-échelon folds and systematically arranged arrays of reverse fault and extension joints controlled by left-lateral movements of this fault system.

The Keumwang fault zone is an exhumed ancient fault of the Kongju fault system. The movement history, displacement, and the depth range from which the fault zone was exhumed are not clear yet. This fault zone is a left-lateral, strike-slip fault zone, 25 km in length and up to approximately 200 m in width. The studied fault segments are relatively well-defined and continuous and strike N 44–65°E with dips 60–85°SE. The northern segment of the Keumwang fault zone borders the Cretaceous Pungam basin

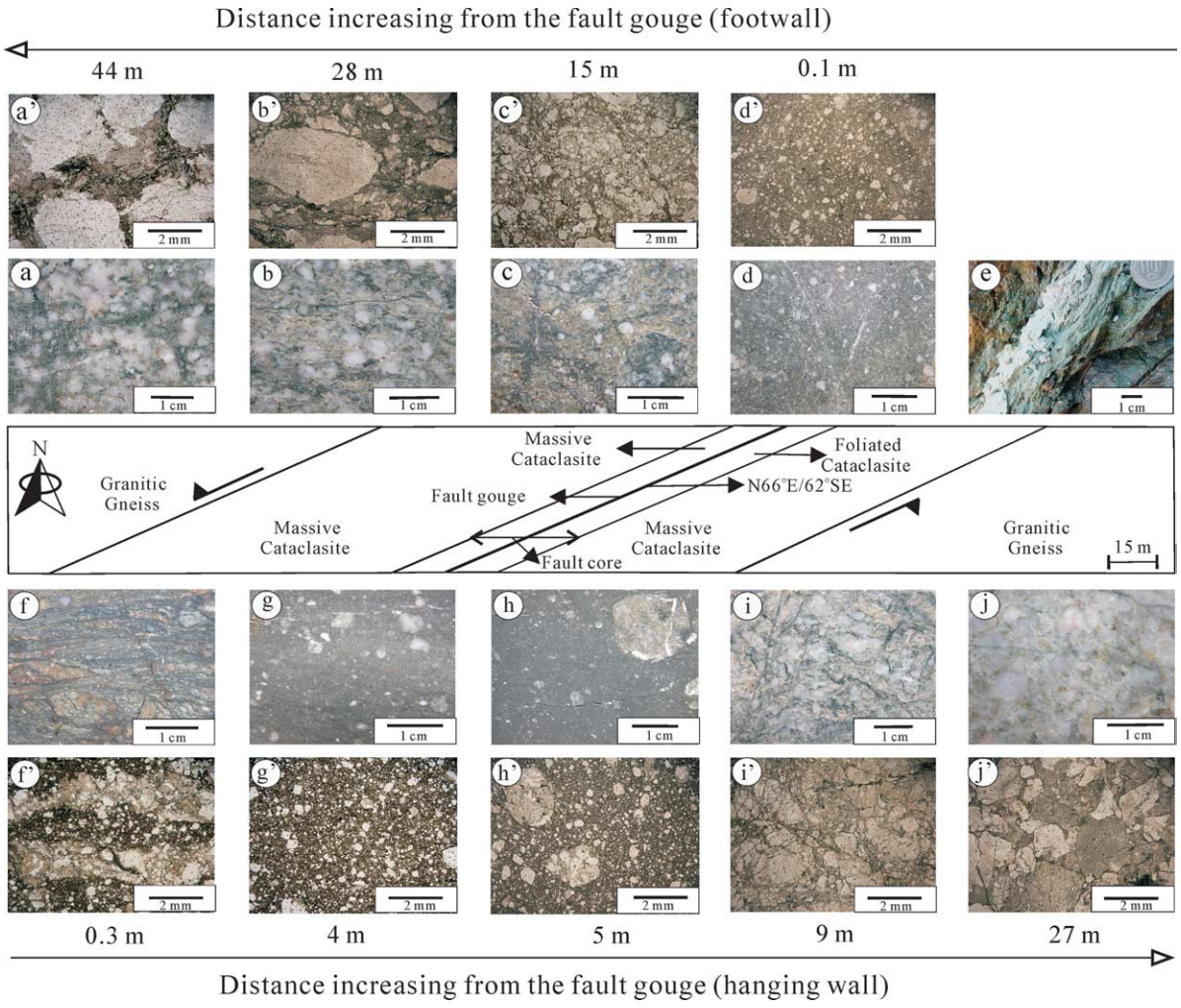

Fig. 2. Schematic map across the Keumwang fault zone illustrating distribution of the fault rock type and internal structures of the fault zone at location A. (a) to (j) are photographs of rock slabs; (a-1) to (j-1) are photomicrographs. (a), (a′), (j), (j′): host rock; (b), (c), (b′), (c′): cataclasite in footwall, (d), (f), (d′), (f′): cataclasite in fault core; (f), (f′) show cataclasitic foliations, indicating multiple episode of cataclasitic flow. (g), (h), (i), (g′), (h′), (i′): cataclasite in hanging wall. All photomicrographs are in plane-polarized light. The amount of fine-grained matrix increases and the size of the porphyroclasts decreases toward the fault gouge.

filled with a sequence of conglomerate, sandstone and mudrock. Three locations were studied along the northern segment of the Keumwang fault zone where Cretaceous sedimentary rock, andesite and basement are juxtaposed. One location was studied along the southern segment of the Keumwang fault zone where it occurs within the Precambrian granitic gneiss. The basement consists of granitic gneiss and two-mica granite, granodiorite and leucocratic granite and biotite granite. The Cretaceous sedimentary rock consists of an interbedded sequence of conglomerate, sandstone and mudrock. Quartz porphyry intrudes these rocks. Structural features associated with fault movements are developed both in the granitic gneiss and mudrock.

3. Mesoscopic structure of the Keumwang fault zone

3.1. Structure of fault in crystalline rock (location A)

The fault zone at location A, in the southern segment of the Keumwang fault zone, occurs in Precambrian granitic gneiss and is approximately 80 m in thickness. The fault zone is composed of a fault core and a zone of damaged host rock containing massive cataclasite (Fig. 2). The fault core consists of a 2–7-cm-thick fault gouge layer (Fig. 2e) bounded by a zone of 4-m-thick foliated cataclasite (Fig. 2f and f′) on the hanging wall side and about 4-m-thick massive cataclasite (Fig. 2d and d′) on the footwall side

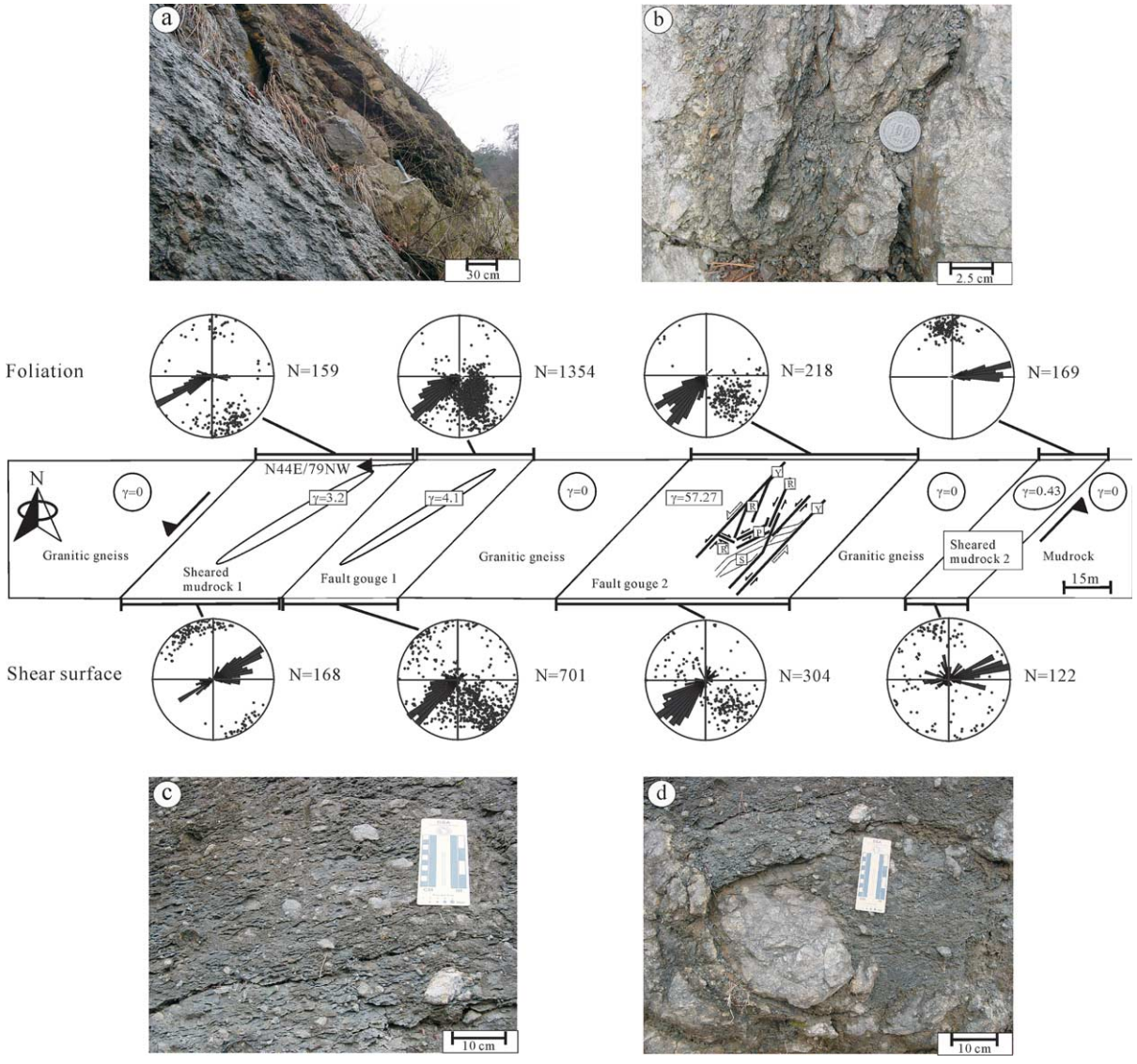

Fig. 3. Schematic map across the Keumwang fault zone showing the internal structures of the fault zone at location B. Shear strains (γ) determined by the relationship between the orientation of foliation and shear direction are included. The fault zone consists of sheared mudrock 1 and 2, fault gouge 1 and 2 derived from granitic gneiss, and two slivers of granitic gneiss. The directional nomenclature and geometrical relationships of the structural elements follow Rutter et al. (1986) and Passchier and Trouw (1996). Stereonets are lower hemisphere, equal area projections of poles to foliations and shear surfaces. Rose diagrams of the strike of foliations and shear surfaces are included. Photographs of the outcrops: (a) slivers of undeformed granitic gneiss in the fault gouge; (b) fragments of the protolith; (c) foliated fault gouge; (d) older fault breccia within the fault gouge.

(Fig. 2). The average orientation of fault surfaces bounding the fault gouge layer is N 66°E and 62°SE at this location.

The fault gouge layer can be divided into two bands of different colour: pale grey and pale greenish grey (Fig. 2e). Foliation subparallel to the fault surface is generated by preferred alignment of clay minerals in the pale greenish grey fault gouge band (Fig. 2e).

The foliated cataclasite in the hanging wall side is defined primarily by the presence of *P*-, *Y*- and *R*-shear bands (Fig. 2f). The shear bands occur as braided or anastomosing networks bounding lens-shaped domains of low strain (Fig. 2f). Shear sense of the shear bands is consistent with sinistral movements of the fault zone. The massive cataclasite in the footwall side is defined by increased amount of the fine-grained matrix (Fig. 2d and d′). Rounded porphyroclasts of older cataclasite are suspended in the fine-grained matrix (Fig. 2d and d-1).

The zone of damaged host rocks consists of about 70 m of massive cataclasite. The massive cataclasite is primarily characterized by a fine-grained matrix derived from the protolith (Fig. 2b, b′; c, c′; g, g′; h, h′; i, i′). The boundary between massive cataclasite and host granitic gneiss is gradational. The massive cataclasite also contains rounded porphyroclasts of several millimetres to 2 cm in diameter. The size and amount of porphyroclasts decrease towards the fault core (Fig. 2).

3.2. Structure of fault between crystalline rock and mudrock (location B)

The fault zone at location B juxtaposes granitic gneiss and sedimentary rock. The fault zone consists of two gouge-dominated slivers, two slivers of lenticular undeformed granitic gneiss, and two sheared mudrock layers (Fig. 3). The granitic gneiss slivers range from 50 to 40 m in thickness, and appear to have remained relatively rigid at the time of fault activity (Fig. 3a). The shear surface between the gouge and undeformed granitic gneiss is extremely sharp (Fig. 3a). Extensive reworking of the fault rocks is indicated by the presence of fragments of older fault breccia suspended in the foliated gouge (Fig. 3b and d). Although a part of the gouge at this location appears to be characterized by an increased amount of included fragments in various stages of breakdown, the intensity of development of the foliation is relatively uniform throughout the whole gouge-dominated layer (Fig. 3c).

The mudrock outside of the fault zone is massive but contains penetrative *S*-foliations and discrete shear surfaces between *P*- and *Y*-shear directions within the sheared mudrock in the fault zone. The orientation data of planar structures in the fault zone at location B are summarized in Table 1. Relative to the orientation (N44°E/79°NW) of the main fault surface between the sheared mudrock and protolith of granitic gneiss, foliations in mudrock layer 2 are in the *P*-shear direction and those in mudrock layer 1 are in the *Y*-shear direction. These foliations could be referred to as *P*-foliation (Rutter et al., 1986) or *S*-foliation (Passchier and Trouw, 1996), which develops in an orientation between 135 and 180° to the shear direction. We assume foliations in the fault zone generally reflect the S_1S_2 plane of the finite strain ellipsoids, and were rotated towards the fault zone orientation with an increase in shear strain (Ramsay and Huber, 1983; Chester and Logan, 1987; Davis and Reynolds, 1996). If correct, the bulk shear strain determined by relationships between the shear direction and the orientation of foliation is about 3.2 for the mudrock layer 1 and 0.43 for the mudrock layer 2 indicating that shear strain is greater near the sharp northwestern boundary between granitic gneiss and mudrock than near the gradational southeastern boundary within the mudrock. The dip of the foliation has a tendency to steepen towards the centre of the fault gouge layers (Fig. 3). The bulk shear strain estimated by relationships between the shear direction and the orientation of foliations is about 4.1 for the gouge layer 1 and about 57 for the gouge layer 2, which are much greater than those of the sheared mudrock (Table 1 and Fig. 3).

The distributions of shear surfaces range between *Y*- and *P*-shear directions in the sheared mudrock and gouge layers (Table 1 and Fig. 3). Dominant shear directions in each layers correlate with shear strain estimates. *Y*-shear direction is dominant in the gouge layers with greater strain

Table 1
Domain of rock type and summary of orientation data of planar structures in the fault zone at location B

Domain	Shear surface				Foliation				
	Range	Mean	Deviation (°)	Shear direction	Range	Mean	Deviation (°)	Shear direction	Shear strain
Sheared mudrock 1	N40°E–EW	N66°E/ 84°SE	22	*Y*	N45°E–N80°E	N75°E/ 75°NW	17	*Y*	3.2
Sheared mudrock 2	N65°E–EW	N67°E/ 78°SE	32	*Y*	N70°E–EW	N83°E/ 70°SE	9	*P*	0.43
Gouge 1	N30°E–EW	N59°E/ 55°NW	27	*Y*	N20°E–N80°E	N55°E/ 32°NW	23	*Y*	4.1
Gouge 2	N25°E–N60°E	N48°E/ 56°NW	24	*Y*	N25°E–N60°E	N42°E/ 49°NW	20	*Y*	57.27

The directional nomenclature of the structural elements follows Rutter et al. (1986) and Passchier and Trouw (1996).

and *P*-shear direction is dominant in the sheared mudrock layers with less strain (Table 1 and Fig. 3).

3.3. Structure of fault between crystalline rock and mudrock (location C)

Location C contains two fault zones separated by about 330 m. Fault zone I juxtaposes the Precambrian granitic gneiss and the Cretaceous mudrock (Fig. 4). The main surface of Fault I is extremely sharp, strikes N 67°E and dips 65°SE and demarcates the contact between fault rocks derived from the granitic gneiss and the sheared mudrock derived from the massive mudrock (Fig. 4a).

An 8-m-thick zone in the crystalline gneiss is defined by alternating gouge and breccia-dominated layers about 40–50 cm thick (Fig. 4b). Discrete shear surfaces and shear bands are developed within the breccia-dominated layers but penetrative foliations are developed in the gouge-dominated layers (Fig. 4c and d). Shear surfaces and shear bands at the boundary between the breccia and gouge-dominated layers appear to accommodate much more shearing than those along foliations (Fig. 4b).

An approximately 40-m-thick damaged zone exists on the hanging wall side of Fault I in which penetrative foliations and discrete shear surfaces are developed in the sheared mudrock. The density of shear surfaces is gradually lowered to the boundary between the damaged zone and protolith of massive mudrock.

The orientation data of planar structures in each domain at location C are summarized in Table 2 and Figs. 4 and 5. The strike of *S*-foliation developed in the fault gouge derived from the granitic gneiss ranges between N 65°E and E 75°W. The orientation-distribution of *S*-foliations is bimodal at both boundaries of the mudrock of the fault

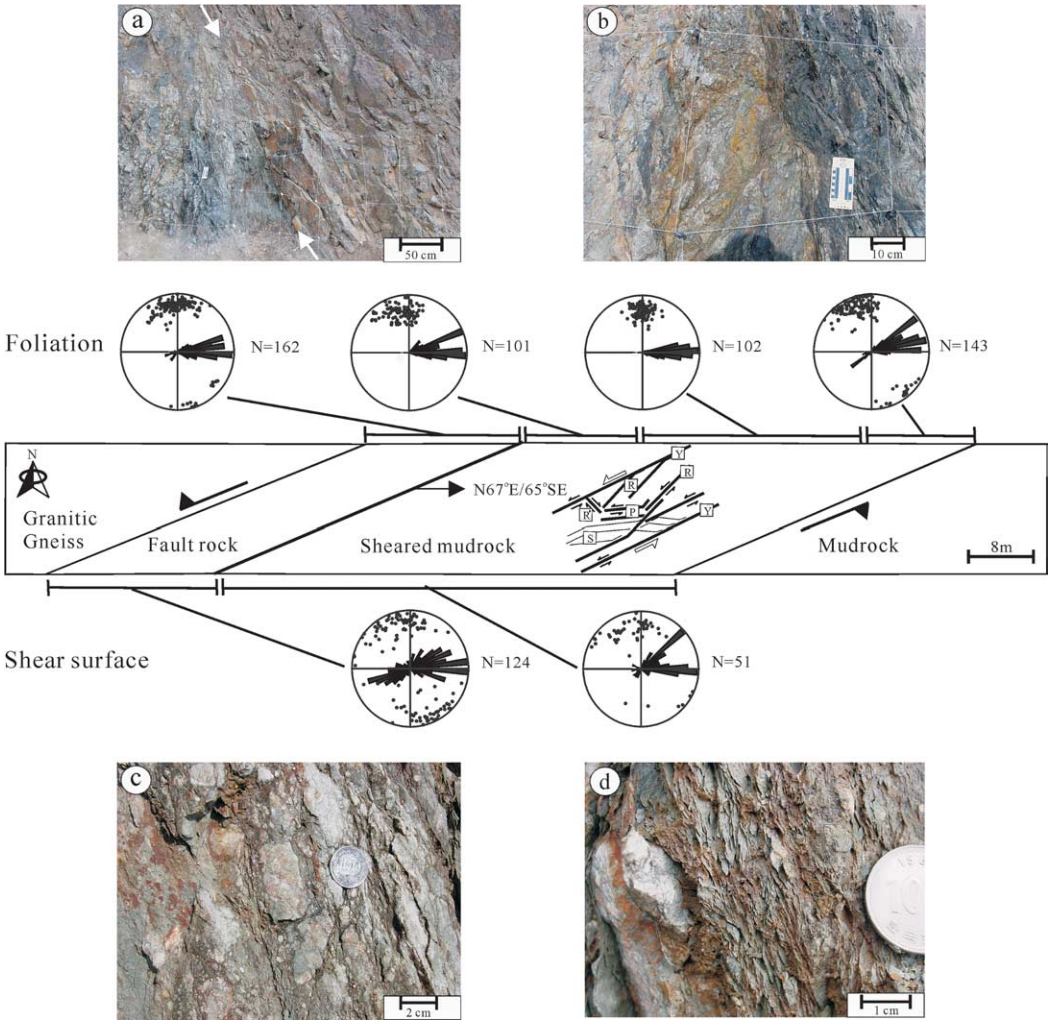

Fig. 4. Schematic map across the Keumwang fault zone showing the internal structures of the fault zone I at location C. Directional nomenclature, geometrical relationships of the structural elements, and stereonets as in Fig. 3. Photograph of the outcrops: (a) fault surface between the sheared mudrock and fault rock derived from gneiss. Small white arrows identify the fault surface between fault rock derived from granitic gneiss and sheared mudrock; (b) fault gouge-dominated layer on right and fault breccia-dominated layer on left of photo; (c) close-up photograph of fault breccia layer; (d) close-up photograph of fault gouge-dominated layer.

Table 2
Domain of rock type and summary of orientation data of planar structures in the fault zone at location C

Fault	Domain		Shear surface				Foliation				
			Range	Mean	Deviation (°)	Shear direction	Range	Mean	Deviation (°)	Shear direction	Shear strain
Fault 1	Breccia/ gouge		N75°E–N75°W	N85°E/81°SE	5	*P*	N65°E–N75°W	N83°E/74°SE	6	*P*	12.16
			N35°E–N70°E	N50°E/87°SE	8	*Y*					
	Sheared mudrock	NW boundary	N25°E–N60°E	N44°E/72°SE	10	*Y*	N40°E–N80°E	N75°E/66°SE	6	*Y*	50.63
			N75°E–N75°W	N88°W/65°SW	8	*P*	N75°E–N80°W	N89°E/60°SE	4	*P*	6.13
		Centre					N75°E–N80°W	N89°E/64°SE	4	*P*	6.13
		SE boundary					N45°E–N55°E	N49°E/86°SE	4	*R*	9.47
							N70°E–N85°W	N81°E/73°SE	4	*P*	16.09
Fault 2	Sheared mudrock	NW boundary	N45°E–N70°W	N78°E/86°SE	11	*P*	N75°E–N80°W	N87°E/80°SE	4	*P*	
			N80°W–N5°E	N2°W/83°NE	6	*R*					
		Centre	N85°E–N85°W	N88°W/88°SW	3	*P*	N85°W–N70°E	N82°E/87°NW	2	*P*	
			N45°E–N85°E	N67°E/78°NW	6	*Y*					
		SE boundary	N80°W–N75°E	N87°E/80°NW	4	*P*	N75W–N65°E	N81°E/74°NW	5	*P*	
			N45°E–N88°E	N60°E/78°NW	5	*Y*					

Nomenclature as in Table 1.

zone I. The strike of the *S*-foliation in the central part of the mudrock is predominantly in the direction of *P*-shear (Fig. 4).

Shear surfaces and shear bands of *Y*-shear direction are predominant and subparallel to the trace of the host fault zone. The next dominant orientation of shear surfaces and shear bands is *P*-shear direction (Table 2 and Fig. 4).

Fault zone II is about 25 m thick and defined by the presence of foliations in the sheared mudrock bounded by the massive mudrock. Both boundaries of the fault zone are obscured by intrusion of a felsic dyke. The orientation of *S*-foliations is unimodal at each location across the fault zone. The dip of the foliation is quite steep and the dip direction is changed from NW in the southeastern area to SE in the northwestern area across the fault zone (Table 2 and Fig. 5).

The orientation of shear surfaces is varies systematically in fault zone II. *P*- and *R*-shears are dominant at the northwestern area of the fault zone. Shear surfaces between

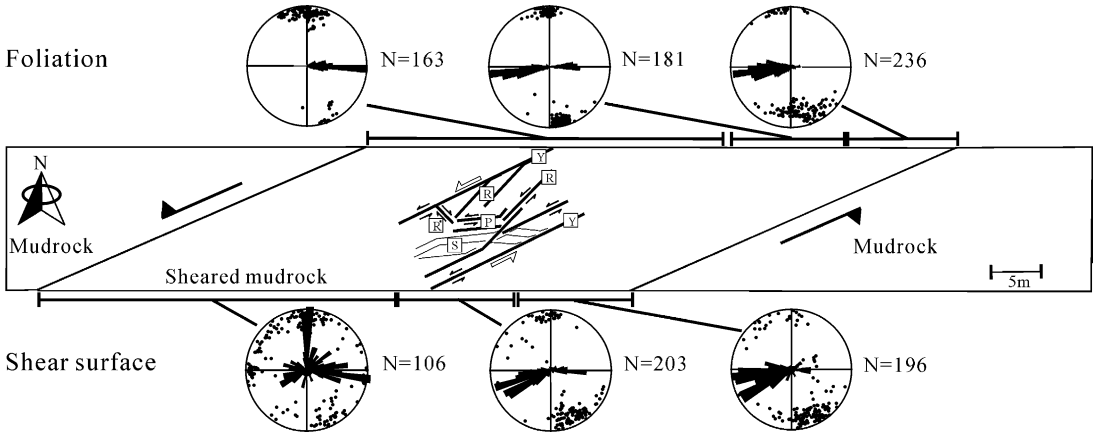

Fig. 5. Schematic map across the Keumwang fault zone showing the internal structures of the fault zone II at location C. Nomenclature and stereonets as in Fig. 3.

P- and *Y*-shear directions are developed at the southeastern area of the fault zone (Table 2 and Fig. 5).

3.4. Structure of fault between crystalline rock and mudrock (location D)

The extremely sharp fault surface at location D is located between the foliated cataclasite of granitic gneiss and the sheared mudrock (Fig. 6a). The fault zone strikes N 54°E and dips 70°SE and a fault core is not evident at this location. Cataclastic foliations are dominant within a 4-m-thick damaged zone of granitic gneiss and their orientations are subparallel to the fault surface (Fig. 6b). Quartz and feldspar grains are microfractured (Fig. 6e) and shear bands are developed (Fig. 6f).

Sheared mudrock has anastomosing *S*-foliations with high dip angle (70–90°) that surround massive ellipsoidal pods of several centimetres to metres in diameter (Fig. 6c). The amount and size of unsheared ellipsoidal pods tends to decrease toward the main fault surface. Pale greenish brown-coloured sheared mudrock alternates with purple-coloured sheared mudrock (Fig. 6d). The surfaces separating these must be regarded as *Y*-shear surface. Andesite intruded into the sheared mudrock near the southeastern boundary and then the fault was reactivated resulting in a fault contact between the sheared mudrock and andesite. There are no structural features related to faulting within andesite at this location.

The orientation data of structural elements in the fault zone at location D are summarized in Table 3. *S*-foliations show systematic variations in orientation within the fault zone (Fig. 6). They are rotated subparallel to the main fault surface near the northwestern boundary of the fault zone reflecting the highest shear strain within the fault zone (Table 3 and Fig. 6).

The distribution of shear surfaces also varies

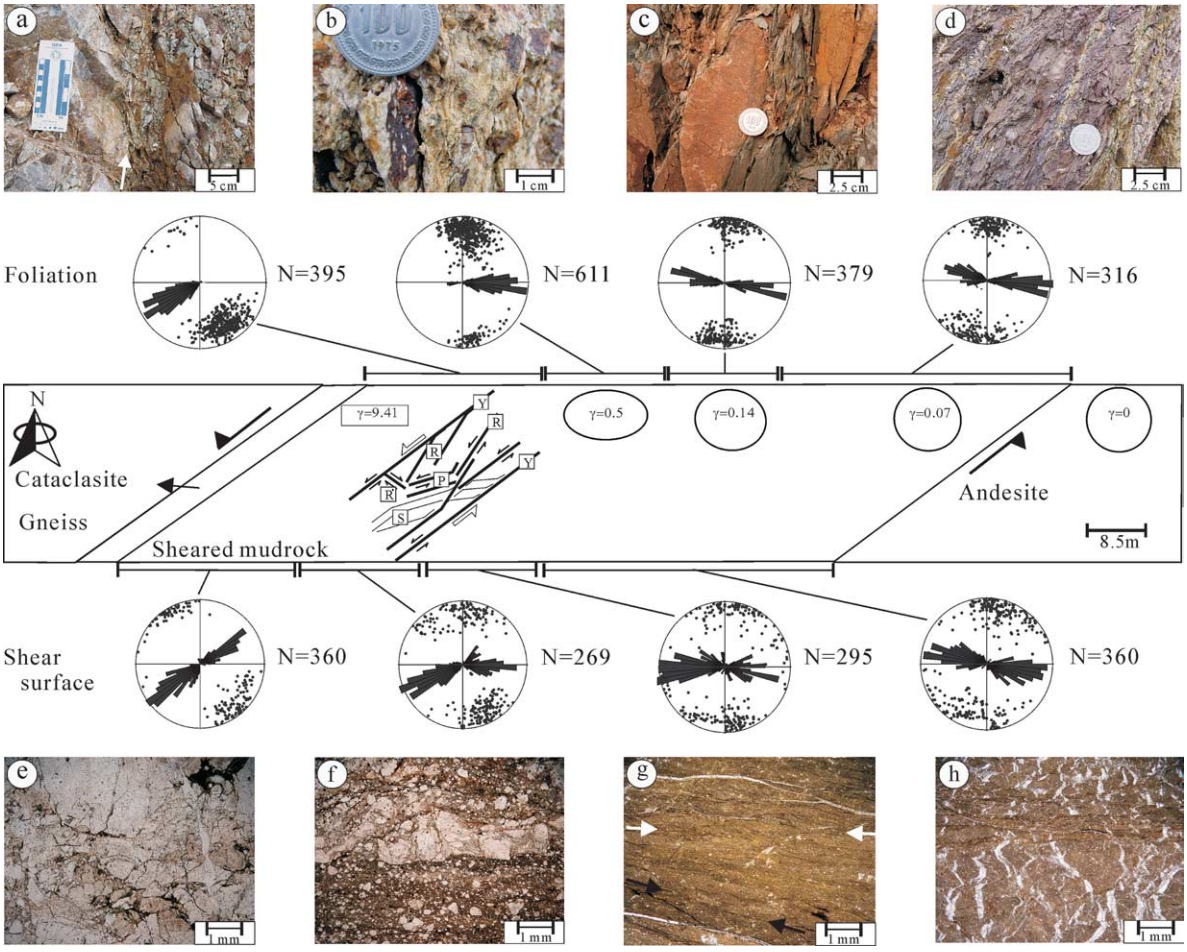

Fig. 6. Schematic map across the Keumwang fault zone showing the internal structures of the fault zone at location D. Shear strains (γ) determined by the relationship between the orientation of foliation and shear direction are included. Nomenclature and stereonets as in Fig. 3. Photograph of outcrops: (a) fault surface between cataclasite and sheared mudrock. Small white arrows identify the contact between the cataclasite derived from granitic gneiss and the sheared mudrock; (b) close-up photograph of the foliated cataclasite derived from granitic gneiss; (c) lenticular undeformed relics of mudrock within the sheared mudrock; (d) close-up photograph of the sheared mudrock. Photomicrographs of (e) cataclasite; (f) foliated cataclasite; (g) sheared mudrock: black arrows identify micro-shear bands and *S*-foliations are identified by white arrows; (h) calcite veins perpendicular to the foliation in the sheared mudrock. All photomicrographs are in plane-polarized light.

Table 3
Summary of orientation data of planar structures in the fault zone at location D

Distance (m)	Shear surface				Foliation				
	Range	Mean	Deviation (°)	Shear direction	Range	Mean	Deviation (°)	Shear direction	Shear strain
0–15	N35°E–N70°E	N52°E/83°NW	15	*Y*	N40°E–N80°E	N60°E/65°NW	13	*Y*	4.41
15–25	N35°E–N80°E	N60°E/78°NW	11	*Y*	N75°E–N8°W	N88°W/71°SW	12	*P*	0.5
	N75°E–N70°W	N85°W/79°NE	13	*P*					
25–35	N65°E–N50°W	N84°W/80°NE	23	*P*	N85°E–N70°W	N83°W/88°NE	10	*P*	0.14
35–60	N70°E–N40°W	N75°W/90°	18	*P*	EW–N55°W	N81°W/86°NE	13	*P*	0.07

Nomenclature as in Table 1.

systematically across the fault zone in this location (Fig. 6). *Y*-shears are dominant near the main fault surface and *P*-shears are dominant in the other part of the fault zone (Table 3 and Fig. 6).

4. Microscopic observations and fault rock geochemistry

4.1. Fault in the crystalline rock (location A)

The microstructures and mineral changes of the Keumwang fault zone at location A indicate that cataclasis and alteration were significant at the time of fault movement. Undeformed granitic gneiss in the protolith shows a granular texture with coarse grains (Fig. 2a′ and j′), but this texture disappears gradually toward the fault core (Fig. 2). Rocks in this traverse could be grouped into protolith, massive cataclasite, foliated cataclasite, and fault gouge (Fig. 2). Massive cataclasite in the damage zone consists of porphyroclasts within fine-grained matrix, which is the product of alteration and comminution of protolith (Fig. 2b′–d′ and g′–i′). The amount of fine-grained matrix increases toward the fault core (Fig. 2). The foliated cataclasite within the fault core is composed of fine-grained matrix and porphyroclasts of older cataclasites (Fig. 2f′). Microscopic shear bands in *Y*- and *R*-shear directions are distinguished by very-fine-grained matrix (Fig. 2f′).

The variations of the particle size across the fault zone are shown in a plot of grain-size versus distance from the fault gouge (Fig. 7a). In the host rock, grain-size of quartz and plagioclase is about 3–4 mm on average, and then is dramatically reduced at about 30 m from the fault gouge (Fig. 7a).

Variations in mineral content across the fault zone reflect an apparent gradual increase in alteration toward the fault core. Major minerals of the granitic gneiss are quartz,

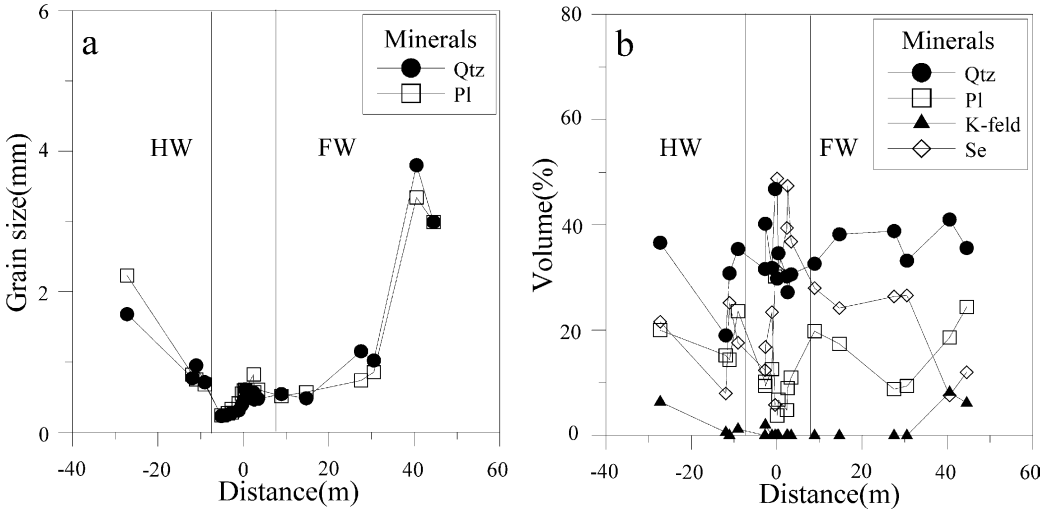

Fig. 7. (a) Variations in mean grain size of quartz and plagioclase measured with a petrographic microscope across the fault zone at location A. (b) Diagram showing the variations of modal composition of the minerals plotted with respect to the distance from the fault gouge. Vertical line indicates the location of the fault core. Mineral abbreviations: Qtz, quartz; Pl, plagioclase; K-feld, K-feldspar; Se, sericite.

plagioclase, sericite, chlorite, with minor minerals including biotite, calcite, K-feldspar (microcline and perthite), and opaque minerals. Massive cataclasite bounding the fault core is composed of fine-grained matrix, quartz, plagioclace, sericite and porphyroclasts of quartz and rock fragments. The foliated cataclasite within the fault core is composed of fine-grained matrix, quartz, biotite, plagioclase, clay minerals and porphyroclasts of older cataclasite. The fault gouge layer is composed almost entirely of small particles of quartz and clay minerals altered from feldspars. Volume variation in modal composition away from the fault gouge is shown in Fig. 7b. Quartz content does not show distinct change across the whole fault zone, but sericite increases toward the fault gouge. K-feldspar (microcline and perthite) does not exist within the fault rock zone, but occurs only in the protolith 35 m away from the fault gouge. Content of plagioclase is less than 10% in the fault core and increases up to 25% in the protolith. These changes in modal composition suggest the introduction and efflux of water and K^+ during fault movements.

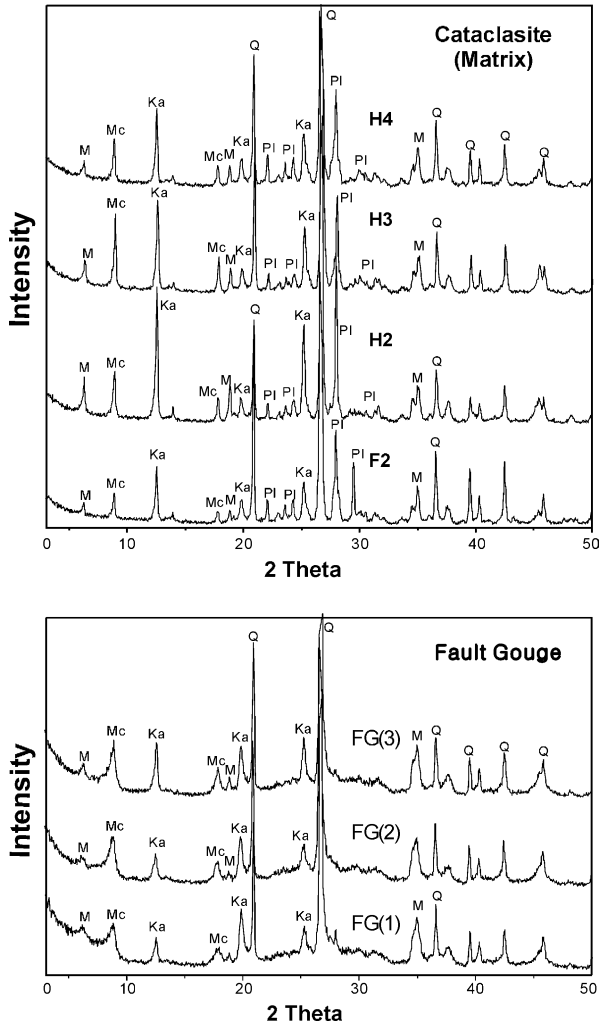

Fig. 8. X-ray diffraction patterns of matrix of cataclasite and fault gouge at location A. Mineral abbreviations: M, montmorrillonite; Mc, mica; Ka, kaolinite; Il, illite; Q, quartz; Pl, plagioclase. Symbols: F2, cataclasite collected from the footwall; H2, H3, H4, cataclasite collected from the hanging wall; FG(1), FG(2), FG(3), fault gouge collected from the central fault gouge layer.

Results of XRD analysis provide more detailed information about the appearance and demise of minerals in the fault core. Matrix of the cataclasite is composed of illite, montmorillonite, kaolinite, plagioclase, quartz and mica, which are identical to the mineral composition of the fault gouge layer, except for plagioclase, which does not exist in the fault gouge. This indicates that comminution and fluid–rock reactions are dominant in the central fault gouge layer within the fault core during fault movements (Fig. 8).

Results of XRF analysis show variation of major components of fault rock reflecting chemical reaction and solute transport and deposition (Fig. 9). The fault core is enriched in Al_2O_3, K_2O, P_2O_5, and TiO_2 and is depleted in CaO and Na_2O. Fe_2O_3 and MgO are enriched gradually from the protolith to the fault core. These observations indicate that alteration and solute transport and deposition were concentrated in the fault core.

SEM images of porphyroclasts within the foliated cataclasite show good roundness (Fig. 10). These observations imply that cataclastic flow including grain boundary frictional sliding, rotation of particles and microfracturing is dominant within the fault zone derived from the crystalline granitic gneiss.

4.2. Fault in the mudrock (location D)

The *S*-foliations in the sheared mudrock are generated by the preferred orientation of the detrital clay minerals, which are distinguished by uniform extinction in thin sections (Fig. 6g). Discrete micro-shear bands are observed in thin sections (Fig. 6g). Clay minerals are randomly oriented within some lenticular mudrock (host rock).

The calcite veins occur as (1) veins parallel to foliation with different thickness (Figs. 6g and 11a), (2) perpendicular to foliation within the sheared mudrock (Figs. 6h and 11b). Some of them show an orthogonal pattern. Calcite veins parallel to foliation consists of a central zone of curved calcite fibres reflecting sinistral movement along the foliation during vein formation, and outer zones of calcite fibres perpendicular to the vein walls indicative of opening normal to foliation (Fig. 11a). This internal geometry of the vein indicates two stages of vein formation, an early stage with an oblique opening component and a later stage without. The fibres of the vein perpendicular to the foliations are perpendicular to the walls indicating that the vein opened in a direction parallel to the foliation, reflecting that the strike of the foliation represents roughly the incremental stretching direction. The median line in these veins is centrally and symmetrically disposed in the vein (Fig. 11b).

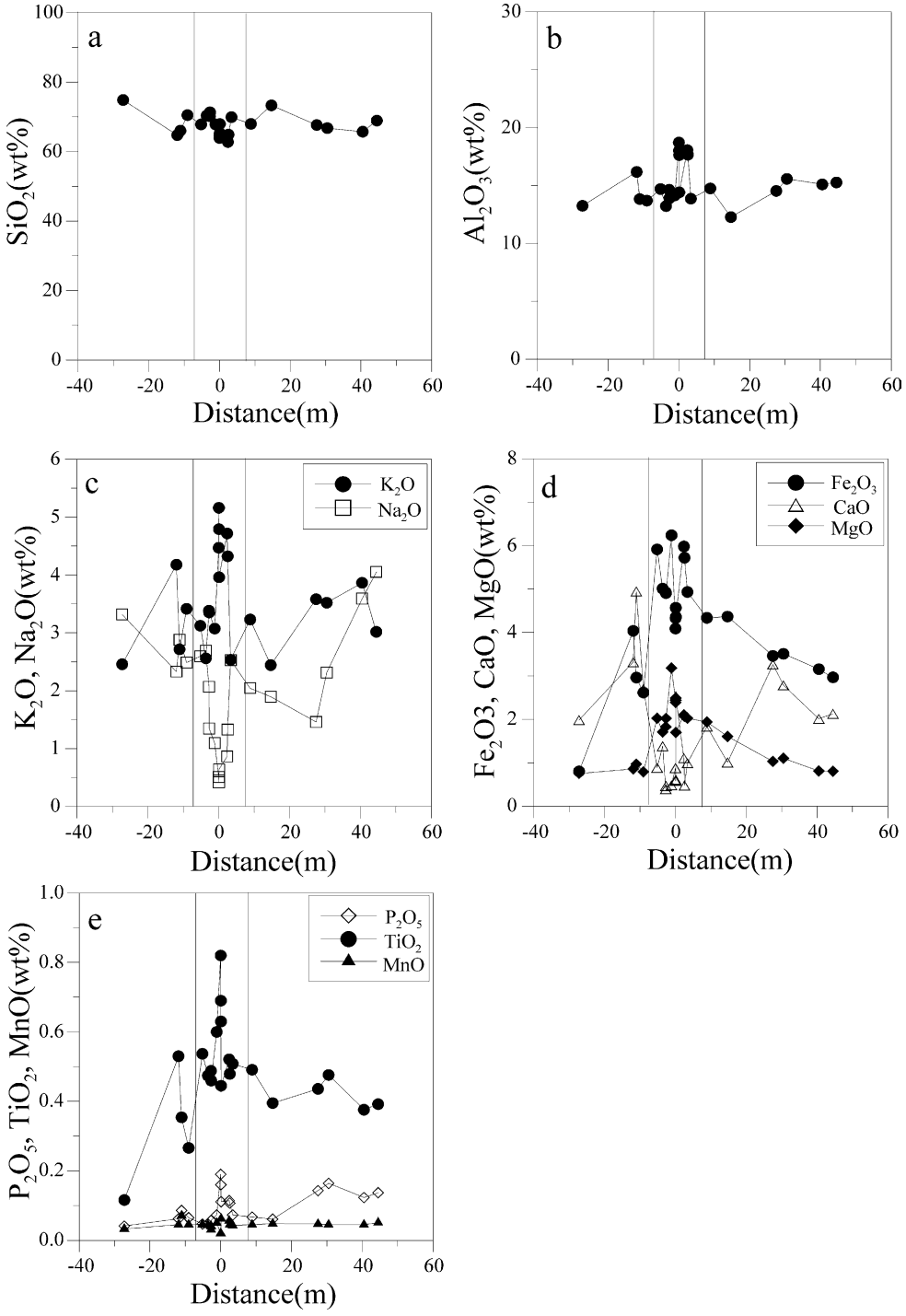

Fig. 9. Spatial variations in the wt% of the measured oxides across the Keumwang fault zone at location A. Vertical line indicates the location of the fault core.

5. Discussion

5.1. Structure of the fault zone in the crystalline rock

Fault breccia, cataclasite and fault gouge are generated by attrition brecciation and distributed crush brecciation (Sibson, 1986) within the fault zone developed in the crystalline granitic gneiss. Cataclastic deformation was partitioned between slip on shear surfaces/shear bands and particulate flow in the fine-grained matrix of cataclasite.

The structure in the fault rock derived from the granitic gneiss records both distributed shear and localized slip at the time of fault activity. At location A, shear deformation was localized at the fault core, which is composed of a fault gouge layer and the foliated cataclasite bounded by the massive cataclasite. Rounded porphyroclasts and lenticular

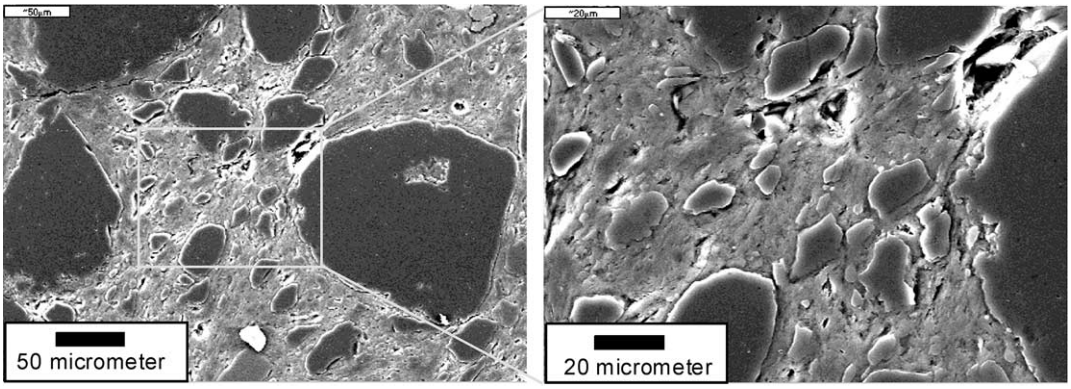

Fig. 10. Scanning electron microscope images of the cataclasite showing the rounded porphyroclasts indicative of frictional grain boundary sliding.

domains of older cataclasite within the fault core indicate reactivation of fault within the fault core by strain softening (Fig. 2f and h′). Strain softening behaviour and mechanisms localizing the zone of deformation in the crystalline rock were described and discussed on the Punchbowl fault and the San Gabriel fault in southern California (Chester and Logan, 1986; Chester et al., 1993; Evans and Chester, 1995; Chester and Chester, 1998). Distributed cataclastic flow was dominant in the damage zone, in which the degree of comminution increases toward the fault core from the host rock.

At locations B and C, the fault zone consists of several gouge-dominated layers, breccia-dominated layers and slivers of relatively undeformed host granitic gneiss. Comminution and alteration were localized in several gouge-dominated layers within the fault zone. The boundary slip surfaces between gouge-dominated layer/breccia-dominated layer and relatively undeformed granitic gneiss appear to be the latest principal surfaces of localized slip (Chester and Logan, 1987; Chester et al., 1993; Chester and Chester, 1998; Faulkner et al., 2003). Wallace and Morris (1986) presented that the Osburn fault in northern Idaho, USA, is composed of one or more gouge zones with anastomosing pattern in a matrix of sheared and foliated rock bordered by highly fractured rock. Fault zones with an anastomosing network of several cores within the damage zone were also described for the Carboneras fault zone within the mica schists in southeastern Spain (Rutter et al., 1986; Faulkner et al., 2003). Faulkner et al. (2003) suggested that strain hardening in the gouge produced a wide fault zone with multiple strands of fault gouge that bound blocks of country rock. In contrast, because the gouge layers cut the shear bands and rock fragments within the breccia, we suggest that strain softening produced an anastomosing network of fault gouge layers within the breccia in the Keumwang fault zone. Lee and Schwarcz (1996, 1999) divided fault zones into type I, II, III and IV modes based on the behaviour of strain hardening and strain softening. They showed that wherever a fault has been reactivated to produce multiple fault gouge-bands, each band exhibits distinct reactivation ages (ESR dates) whose sequence agrees with geological evidence for relative age (Lee and Schwarcz, 1996, 2001).

5.2. Alteration

Although the timing of alteration is uncertain, the formation of phyllosilicate and clay minerals in the fault rock derived from the granitic gneiss appear to be syntectonic. Based on the results of observations of the variations of modal compositions, XRD and XRF analyses across the traverse of the location A, the alteration is

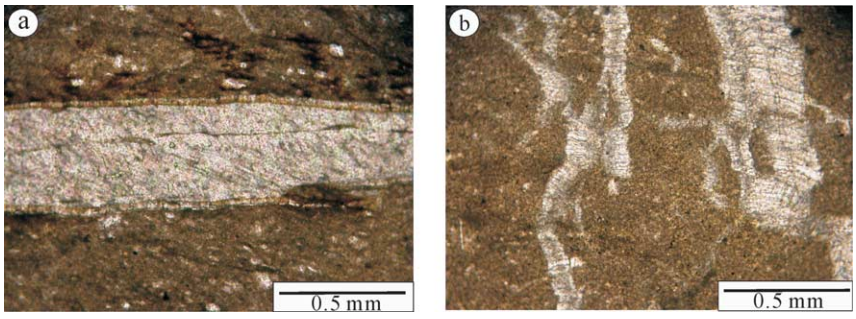

Fig. 11. Photomicrograph of the calcite vein in the mudrock. (a) Calcite fibre vein parallel to the foliation showing curved fibre indicative of sinistral movement. (b) Calcite antitaxial fibre vein perpendicular to the foliation. All photomicrographs are in plane-polarized light.

extremely localized within the fault core, especially within the fault gouge layer, and the most common alteration products are clay minerals (kaolinite and montmorillonite) and phyllosilicates (sericite). The kaolinite is primarily derived from the K-feldspar, plagioclase and mica in granitic gneiss (Evans, 1988; Goddard and Evans, 1995; Wibberley, 1999). Sericite and montmorillonite appear to have resulted from alteration of K-feldspar and plagioclase (Goddard and Evans, 1995). Feldspars are altered to clay minerals by penetration of fluids through microfractures. The grain-size reduction of feldspar within the fault core (Fig. 7a) caused an alteration resulting in reaction-softening. These transformation-induced weakening (reaction-softening) behaviours have been described in several other studies (Evans, 1988; Chester et al., 1993; Evans and Chester, 1995; Wibberley, 1999).

5.3. Structure of the fault zone in the mudrock

Shear deformation is uniformly distributed throughout the whole fault zone developed within the mudrock at outcrop scale. Most of the shear deformation was accommodated by formation of *S*-foliations and then slip along these foliations in the fault zone. Preferred alignment of clay minerals during formation of foliations may occur by rotation and/or mechanisms of controlled oriented growth (Rutter et al., 1986; Chester and Logan, 1987). The former mechanism may have been important at the time of faulting within mudrock, as it already contained detrital clay minerals, and alteration appears insignificant due to lack of feldspar. In contrast, microlithons (lenticular pods) are much less deformed, in which clay minerals are more randomly oriented.

Some displacements are concentrated at discrete shear surfaces of *P*-, *Y*- and *R*-shear orientations in the sheared mudrock. These structural features in the sheared mudrock are similar to structural elements within the Carboneras fault in southeastern Spain, which cut the mica schists (Faulkner et al., 2003). In contrast, the Punchbowl fault, developed within the Pelona Schist in the San Gabriel Mountains, California, consists of one or two fault cores bounded by the damage zone (Schulz and Evans, 1998). The different internal structures between the faults (the Punchbowl and Carboneras faults) cutting through phyllosilicate-rich country rock may be explained by different deformation environments, not by the mechanical properties of the protolith. Because the Keumwang fault zone juxtaposes granitic gneiss and mudrock, we suggest that the different internal structures of this fault zone between mudrock and crystalline gneiss reflect the mechanical properties of the protolith.

The density of shear surfaces is much higher near the main fault surface than in the damage zone of the mudrock. Even though shear surfaces in the fault zone accommodated most of the displacement, the orientation of foliations may reflect qualitatively the bulk shear strain at the early stage of the fault zone evolution at each measurement domain.

6. Conclusions

In this paper we have compared the characteristic structural features, microstructures and geochemistry of the fault zone within different protoliths (granitic gneiss vs. mudrock) along the Keumwang fault zone of the Korean peninsular and made the following observations:

1. The shear deformation tends to be more localized in fault zones cutting the granitic gneiss than mudrock. In gneiss, deformation is partitioned between slip on shear surfaces and bands and particulate flow in the fine-grained matrix of the fault rocks. In mudrock, deformation is accommodated by distributed strain leading to generation of foliation, followed by slip along them.
2. There is a geometric similarity of planar structural features between clay-bearing fault gouge derived from crystalline rocks and sheared mudrock. The *S*-foliation in the clay-bearing fault gouge derived from the crystalline rocks is defined by alignments of phyllosilicates and clay minerals generated by alteration, whereas foliation developed in the sheared mudrock is generated by preferential alignment of detrital clay minerals.
3. The shear surfaces and shear bands are developed predominantly in the *Y*-, *P*- and *R*-shear directions within the fault zone both in the crystalline granitic gneiss and in the mudrock. The shear surfaces transect the *S*-foliations within the fault zone. The stronger the bulk shear strain, the more dominant is the *Y*-shear surface and the more rotated the foliation towards the main fault trace in the sheared mudrock.
4. Alteration increases toward the fault core within the fault zone developed in the crystalline granitic gneiss, whereas little alteration occurred in mudrocks.
5. Wherever the fault juxtaposes the granitic gneiss and mudrock, sharp fault surfaces are developed between fault rock derived from granitic gneiss and the sheared mudrock. They are never mixed.
6. Along-strike variations of characteristic structural features, internal structure of the fault zone and degree of deformation appear to reflect host rock lithology and mechanisms of deformation.

Acknowledgements

This work was supported by Korea Research Foundation Grant (KRF-2000-015-DP0429). An anonymous reviewer

and Dr R.J. Norris are thanked for constructive reviews that improved the paper.

References

Aydin, A., Johnson, A.M., 1983. Analysis of faulting in porous sandstones. Journal of Structural Geology 5, 19–31.

Caine, J.S., Evans, J.P., Forster, C.B., 1996. Fault zone architecture and permeability structure. Geology 24, 1025–1028.

Chester, F.M., Chester, J.S., 1998. Ultracataclasite structure and friction processes of the Punchbowl fault, San Andreas system, California. Tectonophysics 295, 199–221.

Chester, F.M., Logan, J.M., 1986. Implication for mechanical properties of brittle faults from observations of the Punchbowl fault zone, California. Pure and Applied Geophysics 124, 79–106.

Chester, F.M., Logan, J.M., 1987. Composite planar fabric of gouge from the Punchbowl fault, California. Journal of Structural Geology 9, 621–634.

Chester, F.M., Evans, J.P., Biegel, R.L., 1993. Internal structure and weakening mechanisms of the San Andreas fault. Journal of Geophysical Research 98, 771–786.

Chough, S.K., Kwon, S.-T., Ree, J.-H., Choi, D.K., 2000. Tectonic and sedimentary evolution of the Korean peninsula: a review and new view. Earth-Science Reviews 52, 175–235.

Davis, G.H., Reynolds, S.J., 1996. Structural Geology of Rocks and Regions. John Wiley & Sons, New York, USA.

Evans, J.P., 1988. Deformation mechanisms in granitic rocks at shallow crustal levels. Journal of Structural Geology 10, 437–443.

Evans, J.P., Chester, F.M., 1995. Fluid–rock interaction in faults of the San Andreas fault system: inference from San Gabriel fault-rock geochemistry and microstructures. Journal of Geophysical Research 100, 7–20.

Faulkner, D.R., Lewis, A.C., Rutter, E.H., 2003. On the internal structure and mechanics of large strike-slip fault zone: field observations of the Carboneras fault in southeastern Spain. Tectonophysics 367, 235–251.

Flinn, D., 1977. Transcurrent faults and associated cataclasis in Shetland. Journal of the Geological Society of London 133, 231–248.

Goddard, J.V., Evans, J.P., 1995. Chemical changes and fluid-rock interaction in faults of crystalline thrust sheets, northwestern Wyoming, USA. Journal of Structural Geology 17, 533–547.

House, W.M., Gray, D.R., 1982. Cataclasites along the Salville thrust, USA and their implications for thrust-sheet emplacement. Journal of Structural Geology 4, 257–269.

Lee, H.K., Schwarcz, H.P., 1996. ESR plateau dating of periodicity of activity on the San Gabriel fault zone, Southern California. Geological Society of America Bulletin 108, 735–746.

Lee, H.K., Schwarcz, H.P., 1999. ESR dating of multiple gouge layers in a fault zone, Korea. Geological Society of America Abstracts with Programs 31, A-302.

Lee, H.K., Schwarcz, H.P., 2001. ESR dating of the subsidiary faults in the Yangsan fault system, Korea. Quaternary Science Reviews 20, 999–1003.

Mitra, G., 1992. Deformation of granitic basement rocks along fault zones at shallow to intermediate crustal levels. In: Mitra, S., Fisher, G.W. (Eds.), Structural Geology of Fold and Thrust Belts. The Johns Hopkins Studies in Earth and Space Sciences, pp. 123–144.

Passchier, C.W., Trouw, R.A.J., 1996. Microtectonics. Springer, Berlin, Germany.

Ramsay, J.G., Huber, M.I., 1983. The Techniques of Modern Structural Geology, Strain Analysis, vol. 1. Academic Press, London.

Rutter, E.H., Maddock, R.H., Hall, S.H., White, S.H., 1986. Comparative microstructures of natural and experimentally produced clay-bearing fault gouges. Pure and Applied Geophysics 124, 3–30.

Schulz, S.E., Evans, J.P., 1998. Spatial variability in microscopic deformation and composition of the Punchbowl fault, Southern California: implications for mechanisms, fluid-rock interaction, and fault morphology. Tectonophysics 295, 223–244.

Schulz, S.E., Evans, J.P., 2000. Mesoscopic structure of the Punchbowl Fault, Southern California and the geologic and geophysical structure of active strike-slip faults. Journal of Structural Geology 22, 913–930.

Shipton, Z.K., Cowie, P.A., 2001. Damage zone and slip-surface evolution over μm to km scales in high-porosity Navajo sandstone, Utah. Journal of Structural Geology 23, 1825–1844.

Sibson, R.H., 1986. Brecciation processes in fault zones: inferences from earthquake rupturing. Pure and Applied Geophysics 124, 159–175.

Wallace, R.E., Morris, H.T., 1986. Characteristics of faults and shear zones in deep mines. Pure and Applied Geophysics 124, 107–125.

Wibberley, C., 1999. Are feldspar-to-mica reactions necessarily reaction-softening processes in fault zone? Journal of Structural Geology 21, 1219–1227.

Wojtal, S., Mitra, G., 1986. Strain hardening and strain softening in fault zones from foreland thrusts. Geological Society of America Bulletin 97, 674–687.